

A QUANTUM DYNAMIC APPROACH TO THE CONDENSATION PROCESSES OF ZINC ATOMS BY THE INNER-CORE EXCITATION DUE TO ION-RECOMBINATION

Mitsugi Hamasaki^{1*}, Masumi Obara¹, Kozo Obara¹, Hirotaka Manaka¹

¹*Graduate School of Science and Engineering
Kagoshima University, Korimoto 1-21-40, Kagoshima, 8900065, Japan*

(Received: April 2011 / Revised: May 2011 / Accepted: June 2011)

ABSTRACT

Isolated atoms in group II-B such as zinc (Zn), cadmium (Cd), and mercury (Hg) are chemically stable. These atoms are important in the formation of excimer. Zinc in particular has been investigated by many researchers, as Zn₂ excimer holds promise because of its long lifetime and its potential as an energy-storage system. However, excimer's benefits are based on excitation of the outermost electron. Our study confirmed the quantum dynamical condensation processes in which inner-core excitation arises due to ion-recombination between the vapor phase and the solid phase. The X-ray diffraction of the condensed structure of zinc film had included strong diffuse scattering depending on the incident energies. In this research, we produced the excited state of zinc excimer characterized by an extremely long lifetime. Intriguingly, a feature of the zinc film is that it transforms from metallic to insulative. It is thought that such a structure with this characteristic has been affected by electron spin and atomic distortion by inner-core excitation. The structure obtained in our experiment is expected to prove promising in engineering applications, such as electronics, spintronics, and batteries.

Keywords: Bragg reflection; Diffuse scattering; Energy transfer; Inner-core excitation; Surface phase

1. INTRODUCTION

In the vapor phase growth processes, condensation is a most important process in which the translational kinetic energy of incident atoms in the gas phase is dissipated at the crystal surface (Ehrlich & Hudda, 1966). So far, incident energy has been treated as independent from the surface atom system because the surface of the atom system is neutral (Bendavid et al., 2000). In this paper, we propose a method to analyze the quantum dynamic processes in the condensation process from vapor phase to solid phase. We respect the parity of the incident particles. Since the analysis of the particles with the same parity is impossible, we adopted particle systems having different parities. The simplest way to adopt the particles having different parities is obtained by the ionizing in opposite polarities. Normally the lifetime of negative ions is much shorter than that of positive ones (Herzberg, 1944); a unique approach is needed to elongate the lifetime of the negative ions. For this research, a negatively charged crystal surface with electron irradiation was used.

* Corresponding author's email: m-hamasaki@samba.ocn.ne.jp, Tel. +81-99-265-6776, Fax. +81-99-265-6776

The condensation of a positive ion and a negative ion is called the ion-recombination process. The Coulomb force between two ions with opposite polarities produces a strong cohesive force. The translational kinetic energy of the incident ions dissipates at the first collision of these two ions. The most effective process for energy dissipation in this process is the energy transfer from *translational energy to e internal energy* in the ion's electron system.

In order to detect these quantum dynamic processes, we used X-ray diffraction techniques for detecting the spatial correlation between the two atoms. X-ray diffraction intensities clearly depended on the energies of electron irradiation. We found strong diffuse scattering of X-rays on the thin films of zinc deposited by electron irradiation. The strong diffuse scattering indicates the existence of a lattice defect in the thin film observed at the discrete energies of electron irradiation. Further strong Bragg reflection intensities were observed at the discrete energies. These energies correspond to the binding energies of a zinc atom: $3d(10\text{eV})$, $3p(90\text{eV})$, and $3s(140\text{eV})$. These experimental data show the evidence of inner-electron excitation of zinc ions. These electron energies have been dominated by the selection rule of electron transition, $\Delta l = \pm 1$, where l is the orbital angular quantum number. We finally confirmed the existence of unpaired spins in excited zinc atoms by Electron Spin Resonance (ESR). This signal suggests that ion-recombination produces excited states of zinc that appear following ion-recombination and which are characterized by long lifetimes.

2. EXPERIMENTAL

2.1. Experimental system

All experimental procedures were conducted in a vacuum. The vacuum system consisted of conventional equipment including a turbo molecular pump, in which ultimate pressure was 10^{-5} Pa order. Figure 1 provides a schematic illustration of incident electrons, and substrate and zinc ions. The electronic states on the substrates were controlled by the energies of electron irradiation emitted from a cathode in an electron gun. The magnitude of electron emissions was adjusted by the filament current. The kinetic energy of incident electrons was controlled by a potential between the anode of gold thin film deposited around the area of sapphire substrate and the hot filament of cathode in an electron gun. The incident angle of electrons was 45° from the normal substrate surface. Zinc atoms were deposited from the effusion cell, in which the purity of zinc was 99.999%. The zinc atoms were deposited on the insulative area, which measured 6.5 mm in diameter at the center of the substrate.

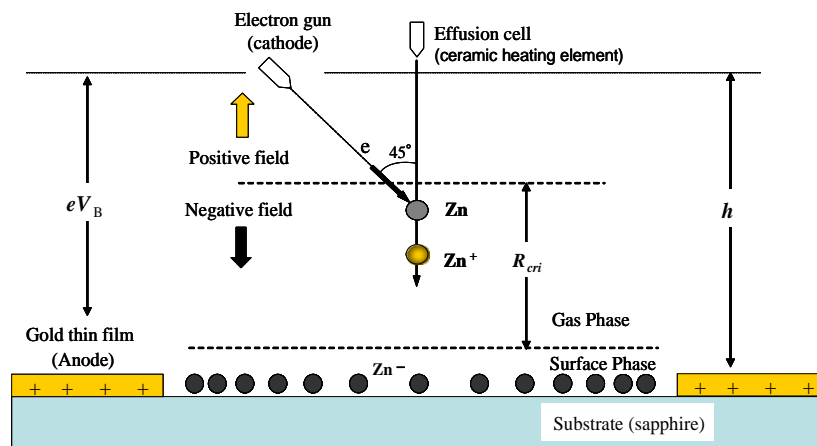


Figure 1 Reaction field with critical point and surface phase

After the anode potential was adjusted to an appropriate level, the first stage was designed to control the potential energy of the insulative area of substrate surface by irradiation of electrons. Electrification in this area is monitored by the transmission electron current measured as the anode current (Obara et al., 2000). This method is one application of “angle resolved transmission electron current spectroscopy” (Obara et al., 1999). After 10 hours from irradiation of the electrons, the electron current became stable at 0.1 μA . The goal of the next stage was to deposit zinc atoms on the substrate surface. The incident angle of the zinc atom beam coming from the effusion cell was held to normal on the substrate surface. As a guide, a typical deposition time of zinc is about 1000 seconds at 600°C in the effusion cell.

2.2. Formation of boundary conditions

The microscopic understanding of growth processes is due to two different concepts of movements: the individual movement of incident atoms and the movement of surface atom systems as a group. The *Surface Phase* is considered to be the region where the two concepts merge (Bird, 1995). A key to controlling the reaction processes in the Surface Phase is the electron states of the surface atom system. The electron states near Fermi energy are complex because the incident atoms in condensation processes are a mix of many electron states that form a new band (Jones et al., 1934). We adopted an approach to the area of the surface phase from the gas phase side, as shown in Figure 1, because it is easy to describe the movement of individual atoms and to make the image of collisions between Zn^+ in the gas phase and Zn^- in the surface phase.

In controllable two-body collision processes, changing of spatial and temporal parameters is a fundamental viewpoint for the generation of new reaction fields. We proposed to decrease the spatial parameters of the reaction field to increase the acceleration of incident Zn^+ just before collision. The magnitude of the acceleration of Zn^+ dominated the interaction with electromagnetic waves in the ion-recombination process. It should be noted that an electromagnetic wave is transformed to interaction energy with electric dipole moments (Ni et al., 2010).

As shown in Figure 1, the Sapphire substrate had a gold electrode for applying the bias voltage for incident electrons. Charged electrons on the insulative area form the negative field and the magnitude of the surface potential, eV_B . This value was equal to the bias potential of the gold electrode. Charged electron density depends on the distance from the center of the circular substrate, and charged electron density near the edge of the circular area was much larger than that at the center of the substrate because of creating homogeneous potential of the substrate. The surface-charged average density, σ_e , and the average distance between the two nearest electrons, d_e , are expressed as follows:

$$\sigma_e = \frac{C_0 R V_B}{\pi R^2} = \frac{C_0 V_B}{\pi R} \quad (1)$$

$$d_e = \left(\frac{e}{\sigma_e} \right)^{1/2} = \left(\frac{e \pi R}{C_0 V_B} \right)^{1/2} \quad (2)$$

where R is the radius of the circular substrate area, C_0 is the coefficient of the capacitance deduced from the experiment, 1.104×10^{-19} F/nm, and e is the electron charge. Since the value, 1.104×10^{-19} F/nm, is equivalent to “ $4\pi\epsilon_0$ ”, we understand that the capacitance of the substrate is equal to the capacitance of the sphere having the same radius. The typical value d_e in the

experiment is a few hundred nanometers. The electric field on the insulative area of the substrate changes the polarity from negative near the surface to positive above the critical point. This critical distance, R_{cri} , is expressed as follows.

$$R_{cri} = \left(\frac{C_0 h R}{4 \pi \epsilon_0} \right)^{1/2} \quad (3)$$

where h is the distance between the anode of the gold thin film and the cathode of the electron gun, and R is the radius of the charged insulative area. The typical R_{cri} of the experiment is several micrometers. The Zn^+ is ionized at the space below the critical point and reacts with Zn^- in the surface phase while explosively accelerating.

2.3. Reaction processes

In the Figure 1, Zn^+ is controlled by the energy of reaction field and reach to Zn^- on the substrate surface. In the early stages, the interaction of both ions is possible to describe as like the dynamic and electromagnetic model which is called direct collision, because the distances between both ions are long. The direct collision process is possible to transfer by high efficiency from total energy to inner energy (Kawazoe et al., 2005).

If the distance between ions approaches at the atomic diameter level, the interelectronic interaction increases in the both ion. In this situation, the linear combination with wave function of Zn^+ and Zn^- make possible to formation of molecular orbital, which is represented by the following equation in a quantum dynamic manner.

$$\psi = (\phi_+ \pm \phi_-) / \sqrt{2(1 - S)} \quad (4)$$

where, ϕ_+ and ϕ_- shows the wave functions of Zn^+ and Zn^- , S indicate the overlap integral between Zn^+ and Zn^- , code \pm distinguish the binding or anti-bonding state of function Ψ . If equation distinguish bonding situation, the condensation process generate the dimer. This dimer makes replacement at position of Zn^- on the substrate.

In order to describe the generation of excimer, our research have required on two important assumptions below (Hatano & Mozumber, 2004).

1. Inner-core electron must be excited before the formation of molecular orbital. If the charge transfer between Zn^+ and Zn^- happens before the formation of molecules, we cannot distinguish between quantum mechanical process because ϕ_+ and ϕ_- became the same wave function.
2. To appear the discrete energy dependence in the measurements of the condensate, inner-core electrons should be excited. In outer electron excitation, the discrete energy dependence does not appear, because outer shell electrons excite to a continuous energy level.

3. RESULTS

3.1. X-ray diffraction

Figure 2 shows the energy dependence of X-ray diffraction intensities scattered from the zinc films deposited under electron irradiation with the energy, eV_B . Strong diffuse scattering of X-rays was observed at inherent electron energies, 10 eV, 90 eV, 100 eV, and 230 eV, which corresponded to the electron binding energies, $3d(10 \text{ eV})$, $3p(90 \text{ eV})$, $3d+3p(100 \text{ eV})$, and $3p+3s(230 \text{ eV})$ of the zinc atoms. Peak profiles at 90 eV, 100 eV, and 230 eV broadened as electron energy increased.

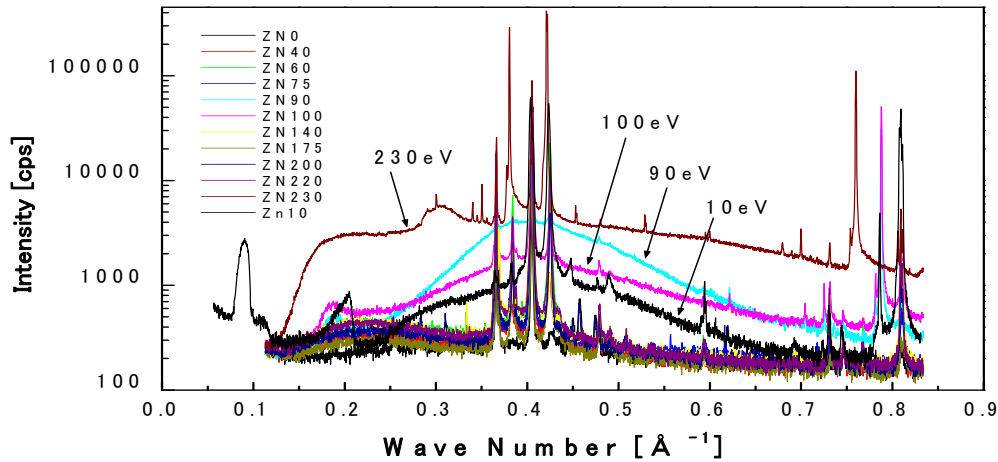


Figure 2 XRD Data showing the diffuse scattering at 10eV, 90eV, 100eV, 230eV

3.2. Diffuse scattering and bragg reflection

Figure 3 highlights the energy dependence of integrated diffuse scattering, illustrated in Figure 2.

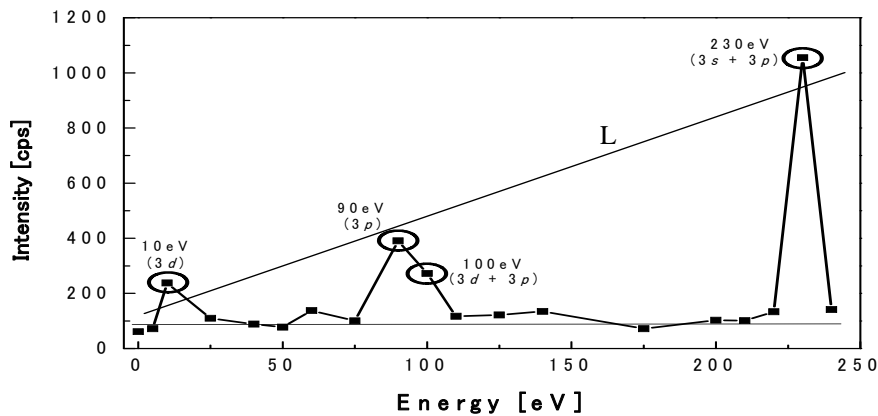


Figure 3 Diffuse scattering

The apparent enhancements of diffuse scattering intensities observed at 10 eV, 90 eV, 100 eV, 230 eV. The intensities of enhanced peaks were approximately proportional to the energy of incident electron as indicated by the line “L”. On the other hand, the electron energy dependence of the peak intensities of Bragg reflection is shown in Figure 4. In this case, the three strong reflection intensities of X-ray were observed at 10 eV, 100 eV, and 140 eV. The scattering intensities linearly increased above 180 eV.

4. CONCLUSION

4.1. Contribution of inner-core excitation

The electron excitation process depends on the initial and the final states in ions. The initial electron states of both ions are $[\text{Ar}]3d^{10}4s^1$ for Zn^+ , and $[\text{Ar}]3d^{10}4s^24p^1$ for Zn^- . The excitation model from the inner-core electron states to the $4s$ -state for Zn^+ , and $4p$ -state for Zn^- , are shown in Figure 5.

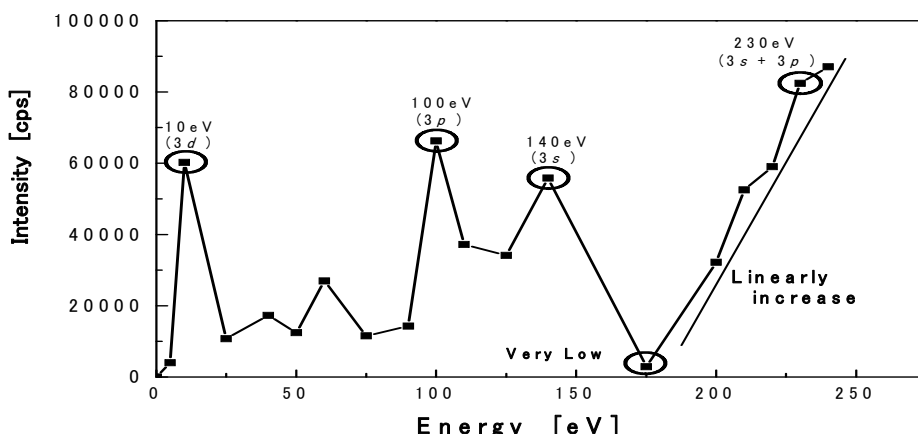


Figure 4 Bragg reflection

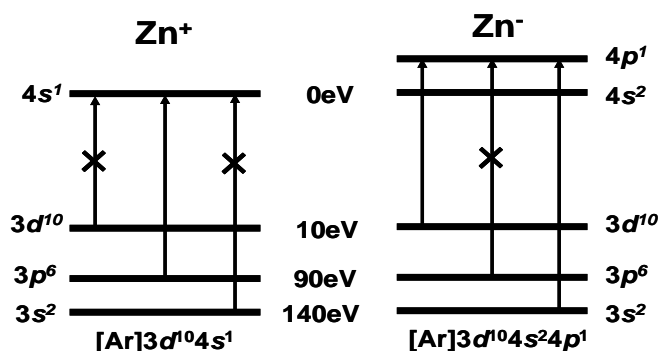


Figure 5 Transition model of Zn⁺ and Zn⁻ according to selection rule

According to the selection rule, $\Delta l = \pm 1$, the 3d-state and the 3s-state in Zn⁻ have the possibility of transitioning to the 4p-state; however in Zn⁺, the 3p-state has only the possibility of transitioning to the 4s-state.

Table 1 shows a summary of discrete electron energy dependence of the scattering intensity of X-rays. The discrete energies include single and double excitations of the inner-core electron states. The energies used are within the range of 0 eV to 240 eV, with the possibility to excite 11 patterns. We classified 3 single excitations as: 10 eV(3d), 90 eV(3p), and 140eV(3s), and 8 double excitations due to the unique combinations of electron states as: 20 eV(3d+3d), 100 eV(3d+3p), 150 eV(3d+3s), 180 eV(3p+3p), 230 eV(3p+3s).

The column marked with "--" has no transitioned ion state. The term "(Zn⁺)*" means the existence of excitation from 3d-state to 4p- state in Zn⁺. The column of "Transition probability" of each ion state is written by numeric "1" for possible cases or "0" for impossible scenarios. The column, "Product of transition probability," means the product of two ions' probabilities. For this reason, numeric "1" shows the strong intensity of diffuse scattering or Bragg reflection and both strong intensities, and "0" shows the weak intensities. The column, "Intensity of diffraction," shows the intensities for diffuse scattering and Bragg reflection, in which characters "H" and "L" mean, respectively, High and Low intensities. The column, "Contribution of excitation," indicates that the "Intensity of diffraction" is affected by excitation of either ion species. The double excitations at 100 eV and 230 eV showed very strong diffuse scattering and Bragg reflection intensity. In the 3 single excitations at 10 eV, 90 eV and 140 eV, both 90 eV and 140 eV showed completely different characteristics.

The transition from the $3p$ -state (90 eV) in Zn^+ produced very strong diffuse scattering and relatively weak Bragg reflection. On the other hand, the transition from $3s$ -state (140 eV) in Zn^- led to strong Bragg reflection only.

Table 1 Transition probability and contribution of transition

Energy (eV)	$\text{Zn}^+(4s)$		$\text{Zn}^-(4p)$		Product of transition probability	Intensity of diffraction		Contribution of excitation	
	State	Transition probability	State	Transition probability		Diffuse	Bragg	Ion species	Excitation
10	--	--	$3d$	1	1	H	H	$(\text{Zn}^+)^*$, Zn^-	Double
20	$3d$	0	$3d$	1	0	L	L	Non	Non
90	$3p$	1	--	--	1	H	L	Zn^+	Single
100	$3p$	1	$3d$	1	1	H	H	Zn^+ , Zn^-	Double
	$3d$	0	$3p$	0	0	L	L	Non	Non
140	--	--	$3s$	1	1	L	H	Zn^-	Single
150	$3s$	0	$3d$	1	0	L	L	Non	Non
	$3d$	0	$3s$	1	0	L	L	Non	Non
180	$3p$	1	$3p$	0	0	L	L	Non	Non
230	$3p$	1	$3s$	1	1	H	H	Zn^+ , Zn^-	Double
	$3s$	0	$3p$	0	0	L	L	Non	Non

We found only one exception at the excitation at 10 eV. The transition from the $3d$ -state (10eV) is possible in Zn^- as shown in Figure 5 and Table 1, which indicates strong Bragg reflection only, but the experimental results showed both strong diffuse scattering and strong Bragg reflection. This contradiction suggests transition from the $3d$ -state to the $4p$ -state in Zn^+ , $[\text{Ar}]3d^9 4s^4 p$ -state, which has 6 excited states with high transition probability from NIST Atomic Spectra Database (Ralchenko et al., 2007). That is, the transition at 10 eV has a competency to give rise to excitation for Zn^- and Zn^+ , respectively. The excitation energies of these states are in the range of 12 eV to 14 eV. The deviation from the bias potential is 2 eV to 4 eV and will be adjusted by the potential difference between Zn^+ and Zn^- . In fact, the electron affinity of Zn^- is approximately zero or negative, and the ionization energy of Zn^+ is 9.39 eV.

If we acknowledge that the transition at the Zn^+ site by 10 eV is due to the above process, then the assumption that the transition at Zn^+ induces strong diffuse scattering while the transition at Zn^- induces strong Bragg reflection completely explains all experimental events or results. These assumptions are perfectly applicable to double excitations at 100 eV and 230 eV in the same way. That is, double excitation at 100 eV includes transition from the $3p$ -state (90 eV) of Zn^+ and at 230 eV includes transition from the $3s$ -state (140 eV) of Zn^- .

4.2. Condensation model

From the discussions of subsections 3.2 and 4.1, authors of this research proposed a model for the condensation process due to the ion-recombination process, as shown in Figure 6. The boundary condition was in the space where Zn^- is located in the surface phase and in the space where Zn^+ was located in the gas phase above the surface phase. As shown in Figure 6(a), the excitation in Zn^+ had an influence on the nearest neighbor, Zn^- . However this excitation was not available to bonding to the Zn atom in the solid phase because of the long distance between Zn^+ in the gas phase and Zn atoms in the solid phase. When the excitation at the Zn^+ site, the bonding with the solid phase became weak. Therefore, Zn^+ and Zn^- have a broad distribution function of lattice spacing for Zn in solid phase, and strong diffuse scattering occur. On the other hand, the excitation in Zn^- influences the two nearest neighbors, Zn^+ and the Zn, as

shown in Figure 6(b). Therefore, when the excitation occurs at the Zn^- site, strong binding with the host crystal is expected, and a strong Bragg reflection is induced.

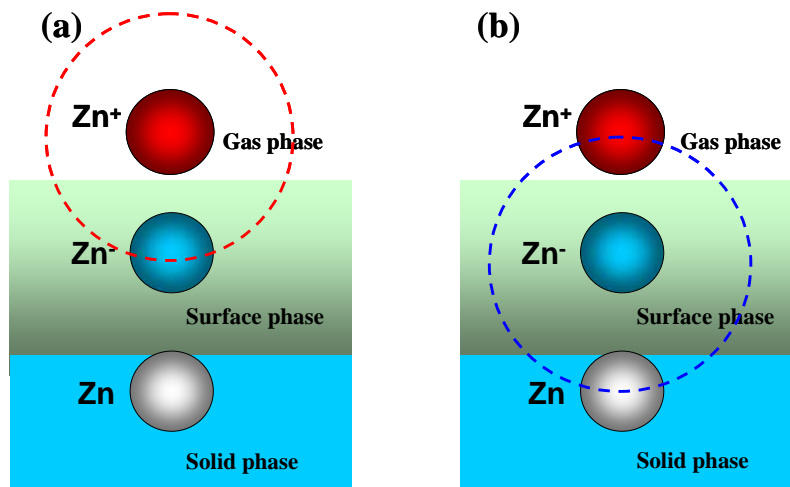


Figure 6 Excitation of: (a) Zn^+ ; (b) Zn^-

Since the diffuse scattering from a metallic substance due to electron irradiation is usually impossible due to the very short lifetimes of the excited states (Itoh & Stoneham, 2000), the observed energy dependent for the strong diffuse scattering of X-rays at room temperature is one proof of the existence of excited states of zinc with a long lifetime (Ernst et al., 1998). The excited states of zinc were confirmed by using the electron spin resonance technique (ESR). The two observed ESR signals suggest the presence of two unpaired electrons: a $3d$ -hole and a $4p$ -electron.

4.3. Mechanism of long lifetime

An existence of the metastable state is essentially important for generating the dimerization with long lifetimes. The mechanisms for long lifetime are as follows. In electron states of the zinc atom, the $4p4s$ -state, just above the $4s$ -state of Fermi level, is the metastable state because its 3P_0 state is not able to transit to ground state 1S_0 by prohibition of the spin-intercombination and selection rule (Haigh, 1995). Another mechanism is to use the stabilization due to dimerization such as H_2 and He_2 . Although hydrogen atoms become stable by forming a bonding state with two stable atoms in which an anti-parallel spin exists in each atom, helium atoms do not form a bonding state because each atom does not have unpaired electrons at ground state. One key for dimerization of zinc is an application of the excited state of helium atoms. The dimerization of helium is only possible when the excited helium atoms combine in accordance with theory on the formation of homonuclear diatomic molecules. This idea is possible to accommodate the dimerization of two zinc atoms, in which one is inner-core electron excited, and the other one is outer shell electron excited (Hay & Dunning, 1976; Xing et al., 1994).

5. CONCLUSION

The quantum dynamic processes for the first step of the condensation process from gas phase to solid phase were investigated by using the ion-recombination process. The electron energy dependencies of the derived crystals showed very strong diffuse scattering at discrete energies, which corresponded to the binding energies of zinc atoms. Strong Bragg reflections were also observed at discrete energies. From the comparison between these two series of experimental data, we proposed a model for the excitation of ions in which the excitation in Zn^+ located at the

gas phase induces strong diffuse scattering while excitation in Zn^- located at the surface phase induces the strong Bragg reflection. This model demonstrates that the inner-core excitation process occurs before the process of charge exchange. We also confirmed the characteristic transformation of zinc film from a metallic to an insulative quality.

6. ACKNOWLEDGEMENT

The authors thank Professor Yosihiko Hatano of the Advanced Science Research Center of Japan Atomic Energy Agency, and Professor Noriaki Itho of Nagoya University for continuous encouragement and helpful discussions.

7. REFERENCES

- Bendavid, A., Martin, P. J., Takikawa, H., 2000. Deposition and Modification of Titanium Dioxide Thin Films by Filtered Arc Deposition. *Thin Solid Films*, Volume 360, pp. 241-249.
- Bird, G. A., 1995. *Molecular Gas Dynamics and the Direct Simulation of Gas Flows*, Clarendon Press, Oxford Engineering Science Series 42.
- Ehrlich, G., Hudda, G., 1966. Atomic View of Structure Self Diffusion: Tungsten on Tungsten. *Journal of Chemical Physics*, Volume 44, pp. 1039-1049.
- Ernst, H. J., Charra, F., Douillard, L., 1998. Interband Electronic Excitation-Assisted Atomic-Scale Restructuring of Metal Surfaces by Nanosecond Pulsed Laser Light. *Science*, Volume 279, pp. 679-681.
- Haigh, C. W., 1995. The Theory of Atomic Spectroscopy; j-j Coupling, Intermediate Coupling, and Configuration Interaction. *Journal of Chemical Education*, Volume 72, pp. 206.
- Hatano, Y., Mozumber, A., 2004. *Charged Particle and Photon Interaction with Matter*. New York (ISBN: 0-8247-4623-6).
- Herzberg, G., 1944. *Atomic Spectra and Atomic Structure*, Inc. New York, 2nd Ed, pp. 229-230.
- Itho, N., Stoneham, A. M., 2000. *Materials Modification by Electronic Excitation*. Cambridge University Press, illustrated edition.
- Hay, P. J., Dunning, T. H., 1976. Electronic State of Zn_2 Ab Initio Calculations of a prototype for Hg_2 . *Journal of Chemical Physics*, Volume 65, Number 7, pp. 2679-2685.
- Jones, H., Mott, N. F., Skinner, A., 1934. Theory of the Form of the X-Ray Emission Bands of Metals. *Physical Review Letters*, Volume 45, pp. 379-384.
- Kawazoe, T., Kobayashi, K., Otsu, M., 2005. Investigation and Development of Optical Near-field Interaction between Nano-materials. *Solid State Physics*, Volume 40, Number 4, pp. 227-238.
- Ni, K. K., Ospelkaus, S., Wang, D., Quémener, G., Neyenhuis, B., M.H.G. de Miranda., Bohn, J. L., Ye, J., Jin, D. S., 2010. Dipolar Collisions of Polar Molecules in the Quantum Regime. *Nature*, Volume 464, pp. 1324-1328.
- Obara, K., Muroya, K., Eguchi, K., Panli, Y., 2000. Angle Dependence of Transmission Probability of Incident Electrons into Thin Oxide Film and Noise Spectra. *Thin Solid Films*, Volume 375, pp. 275-279.
- Obara, K., Chiba, K., Nagano, O., Panli, Y., 1999. Monitoring the Surface Electronic States of Crystals in Vapor-Phase Growth Processes Under Magnetic Field. *Journal of Crystal Growth*, Volume 198/199, pp. 894-899.
- Ralchenko, Yu., Jou, F.-C., Kelleher, D.E., Kramida, A.E., Musgrove, A., Reader, J., Wiese, W.L., Olsen, K., 2007. *NIST Atomic Energy Levels Bibliographic Database for Zn II, NIST Atomic Spectra Database*, Version 3.1.2. National Institute of Standards and Technology Physical Laboratory, Available at: <<http://physics.nist.gov/asd3>>
- Xing, D., Ueda, K., Takuma, H., 1994. Electron Beam Excitation of Zn_2 Excimer. *Japanese Journal of Applied Physics*, Volume 33, Number 12A, pp. 1676-1679.